ACADEMIC PRESS

Available online at www.sciencedirect.com

SCIENCE DIRECT®

Journal of Solid State Chemistry 170 (2003) 237–246

JOURNAL OF SOLID STATE CHEMISTRY

http://elsevier.com/locate/jssc

Exchange interactions in oxovanadium phosphates: towards the understanding of the magnetic patterns

Sébastien Petit,[a,b,*] Serguei A. Borshch,[a,b] and Vincent Robert[a,b,c]

[a] *Institut de Recherches sur la Catalyse, (IRC) UPR 5401, Theorie et Modelisation, 2, Avenue Albert Einstein, 69626 Villeurbanne Cedex, France*
[b] *Laboratoire de Chimie Théorique et des Matériaux Hybrides, Ecole Normale Supérieure de Lyon, 46, Allée d'Italie, 69364 Lyon Cedex 07, France*
[c] *Université Claude Bernard LyonI, 43, Boulevard du 11 Novembre 1918, 69622 Villeurbanne Cedex, France*

Received 28 May 2002; received in revised form 17 September 2002; accepted 7 October 2002

Abstract

We report the calculations of exchange magnetic constants in a series of vanadium phosphorus oxides for which structural and magneto-chemical data are available. Four different types of dimers have been extracted from the crystal lattices in all solids studied. On the basis of a combined density functional theory broken symmetry approach, our calculations on molecular models allow us to define schemes of magnetic interactions. The largest absolute magnetic interaction is provided by the double O–P–O and di-μ-oxo bridges, suggestive of an alternating dimer chain model and an isolated dimer one for the $VO(HPO_4)\cdot 0.5H_2O$ and α-$VO(HPO_4)\cdot 2H_2O$ phases, respectively. Conversely, $VO(HPO_4)\cdot 4H_2O$ is consistent with a bi-dimensional magnetic pattern whereas $VO(H_2PO_4)_2$ and α-$VO(PO_3)_2$ with three-dimensional magnetic schemes. The use of dimer models has been justified by the analysis of higher-nuclearity clusters.

Keywords: Vanadium phosphorus oxides; Magnetic properties; Exchange interactions

1. Introduction

Vanadium phosphorus oxides form a very important solid-state family. For oxovanadium(IV) phosphates, the diversity of magnetic properties has called for a great number of experimental techniques [1–7] and theoretical approaches [8–19]. Oxovanadium(IV) phosphates are characterized by a framework of VO_5 square pyramids linked together. In each unit, the vanadium atom lies above the basal plane resulting in a shorter vanadyl V = O bond with the apical oxygen atom. Two neighboring units can be linked through four different types of connections. Perpendicular to the basal planes, μ-oxo bridges may connect two vanadium sites with one long and one short apical V–O bond. On the other hand, the equatorial oxygen atoms participate in the linkage of two adjacent pyramids by either one di-μ-oxo bridge in a edge sharing way, or by one or two O–P–O bridges. The overall structures may be viewed as arrangements of distorted VO_6 octahedrons and PO_4 tetrahedrons. The various ways in which octahedral and tetrahedral units may be organized give rise to numerous crystallographic structures. These oxovanadium phosphates phases have received much interest from the experimental chemist community since some are known to be precursors of the active catalyst in the synthesis of maleic anhydride from *n*-butane [20–22]. Even though the chemistry of these materials is very similar, different magnetic properties have been observed and very much debated in the literature [1–19]. Indeed, each vanadium site V(IV) being in a d^1 electronic configuration has a local spin of $\frac{1}{2}$. In this class of materials, the richness of exchange pathways between paramagnetic V(IV) centers is responsible for a variety of magnetic interactions. Thus, different magnetic patterns, ranging from nearly isolated dimers to 3-D systems, are observed in different crystal structures.

A major challenge for theoretical chemists is to evaluate the dominating magnetic interactions in order to determine the appropriate interaction scheme. The knowledge of exchange constants is also extremely

*Corresponding author. Institut de Recherches sur la Catalyse, (IRC) UPR 5401, Theorie et Modelisation, 2, Avenue Albert Einstein, 69626 Villeurbanne Cedex, France. Fax: +33-4-72-44-53-99.
E-mail address: spetit@catalyse.univ-lyon1.fr (S. Petit).

0022-4596/03/$ - see front matter © 2002 Elsevier Science (USA). All rights reserved.
doi:10.1016/S0022-4596(02)00114-7

useful in the interpretation of paramagnetic ^{31}P nuclear magnetic resonance (NMR) spectra [23]. On the basis of a combined method including the mapping of exchange constants and a spin model of Heisenberg-type, we were able to extract hyperfine constant values and analyze NMR spectra [15]. Recently, ab initio density functional theory (DFT) calculations [19] have been performed to estimate the magnetic exchange constants in the three reported phases of vanadyl pyrophosphate $(VO)_2P_2O_7$: ambient-pressure orthorhombic (APO), ambient-pressure monoclinic (APM), and high-pressure orthorhombic (HPO). Since the lattice structure of this particular compound was first determined by Gorbunova and Linde [24], much controversy as to the modeling of relevant magnetic interactions has been reported in the literature. The APO phase can be described by the stacking of di-μ-oxo vanadium dimers D_O along the **a** direction resulting in a spin-ladder system (Fig. 1a). The crystal structure along the **c** direction is suggestive of quite another magnetic spin system, an alternating antiferromagnetic dimer chain (Fig. 1b). The latter comes from the alternation of D_O and double O–P–O-bridge dimers D_{OPO}. Surprisingly, the temperature dependence of the magnetic susceptibility has been accurately fitted by both models [8,10]. However, in agreement with very recent experimental fits to inelastic neutron scattering (INS) [11] and light scattering data [18], our calculations of magnetic exchange constants showed that the dimer chain is a valuable starting point [19]. Nevertheless, the assumption of $(VO)_2P_2O_7$ being a strictly one-dimensional dimer chain system was then discarded since our calculations also exhibited a ferromagnetic interchain interaction that should be included when the vanadyl pyrophosphate phases are studied. The comparison of exchange constants calculated in the three phases showed that small variations in distances and angles existing in the crystal structure may lead to significant changes in their strength.

In the mean time, crystallographic structures including the localization of hydrogen atoms and the magnetic properties of five main oxovanadium(IV) phosphates phases have been reported in the literature. These phases exhibit simpler crystallographic unit-cells in comparison to the APM-$(VO)_2P_2O_7$ phase. The $VO(HPO_4)\cdot 0.5H_2O$ [25], α-$VO(HPO_4)\cdot 2H_2O$ [26], $VO(H_2PO_4)_2$ [27] and α-$VO(PO_3)_2$ [28] unit-cells include just one vanadium atom, whereas the $VO(HPO_4)\cdot 4H_2O$ [29] one contains two different vanadium atoms. The magnetic properties of these oxovanadium phosphates have been interpreted on the basis of different models which differ not only in the type of interactions but also in the strength of their coupling constants (Table 1).

The hemihydrate phase $VO(HPO_4)\cdot 0.5H_2O$ is made of dimer chains along the **b**-axis organized in a layered structure (Fig. 2). As in vanadyl pyrophosphate phases, these chains result from the alternation of D_O and D_{OPO} type dimers. In the **c**, direction the stacking results from hydrogen bonding through H_2O molecules and HPO_4^{2-} groups. In spite of the presence of similar patterns, the magnetic interactions models that have been proposed may differ for $(VO)_2P_2O_7$ and $VO(HPO_4)\cdot 0.5H_2O$. As a main result, an isolated dimer picture was suggested to fit the magnetic susceptibility [3] and INS experimental

Table 1
Experimental exchange parameters in different oxovanadium phosphates

Solid	J(K)	References	Dimer types
$VO(HPO_4)\cdot 0.5H_2O$	88.0	[1]	D_O, D_{OPO} and M
	86.0	[3]	
	90.6	[6]	
α-$VO(HPO_4)\cdot 2H_2O$	46.0	[30]	D_{OPO}, M and O
$VO(HPO_4)\cdot 4H_2O$	9.4	[30]	D_{OPO} and M
	13.0	[2]	
$VO(H_2PO_4)_2$	4.4	[3]	M and O
α-$VO(PO_3)_2$	3.5	[31]	D_{OPO} and O

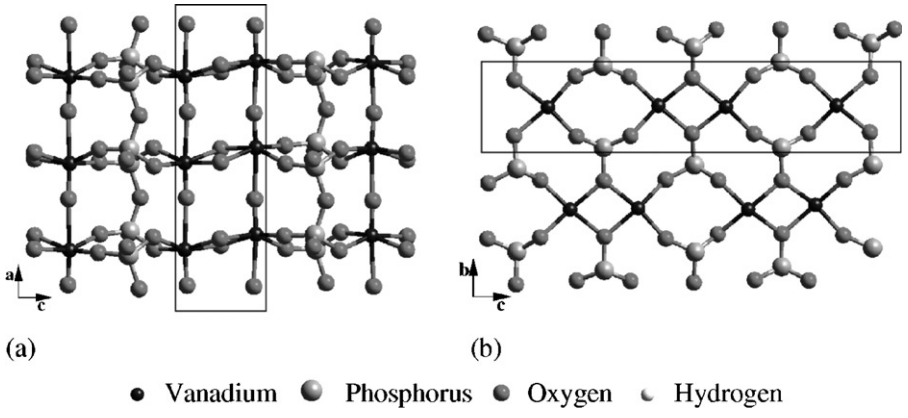

Fig. 1. (a) $(VO)_2P_2O_7$ spin-ladder structure along the **a** direction in the APO phase. (b) Alternating dimer chain along the **b** direction. The rectangles show the constitutive dimeric units.

data [6] for $VO(HPO_4)\cdot 0.5H_2O$. Extended Hückel (EH) calculations of the energy gap between the singly occupied molecular orbitals suggested that the dominant pathway should occur along D_O dimers [12]. Conversely, the INS studies supported another intrachain exchange mechanism involving the double O–P–O bridges. Very recently, the $(VO)_2P_2O_7$ phase [32,33] and its precursor $VO(HPO_4)\cdot 0.5H_2O$ have been synthesized along with high-precision crystal structures analysis [33]. EH calculations revealed that the di-μ-oxo interaction dominates over the double O–P–O interaction.

Apart from $VO(HPO_4)\cdot 4H_2O$, all other phases also exhibit lamellar structures. For the α-$VO(HPO_4)\cdot 2H_2O$ compound, neighboring layers interact by means of hydrogen bonding (Fig. 3). Each layer consists of HPO_4 groups sharing μ-oxo chains organized along the **b** direction. Both magnetic susceptibility and electron spin resonance (ESR) [30] data suggested that α-$VO(HPO_4)\cdot 2H_2O$ solid behaves as isolated antiferromagnetic dimers, attributed to interchain D_{OPO} dimers [12].

In $VO(H_2PO_4)_2$ and α-$VO(PO_3)_2$ solids, VO_5 pyramids are stacked along the **c**- and **b**-axis, respectively, giving rise to linear chains of vanadium atoms (Figs. 4a and b). The μ-oxo chains are connected by single and double O–P–O bridges in $VO(H_2PO_4)_2$ and α-$VO(PO_3)_2$, respectively. For both compounds, fits of the temperature-dependent magnetic susceptibility are consistent with an antiferromagnetic chain model. The extracted small antiferromagnetic constant was assigned to intrachain μ-oxo dimer O [3,31].

The crystal structure of $VO(HPO_4)\cdot 4H_2O$ is indicative of a different pattern, since pairs of dimer chains system along the **a** direction may be considered (Fig. 5). Within this picture, each chain consists of singly O–P–O bridged dimers M, connected to one neighboring chain shifted by half a lattice vector **a**/2. If one looks into the interchain interactions, the association of D_{OPO} units can be viewed as one zigzag chain of vanadium atoms. The magnetic susceptibility data have been fitted by a linear antiferromagnetic dimer chain model, consistently with the zigzag chain picture [2,3].

In this paper, we intend to give some insights into the understanding of magnetic properties in a variety of oxovanadium (IV) phosphates. Our goal is to bridge the

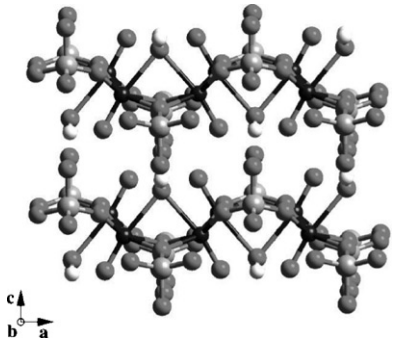

Fig. 2. Hemihydrate $VO(HPO_4)\cdot 0.5H_2O$ structure.

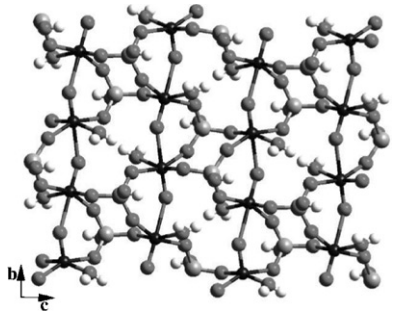

Fig. 3. Structure of the α-$VO(HPO_4)\cdot 2H_2O$ solid. The water molecules are not shown in this figure.

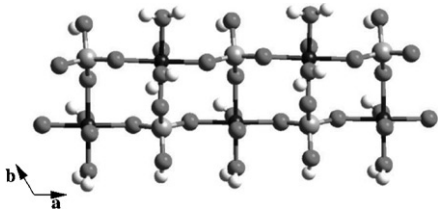

Fig. 5. Tetrahydrate $VO(HPO_4)\cdot 4H_2O$ structure. The water molecules are not shown in this figure.

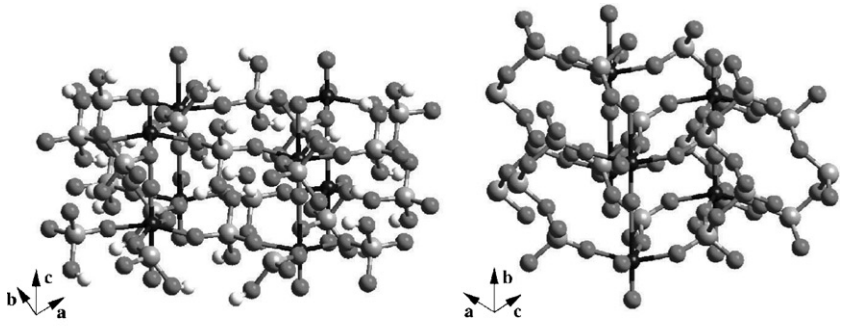

Fig. 4. Structures of the $VO(H_2PO_4)_2$ (a) and α-$VO(PO_3)_2$ (b) compounds.

gap between exchange constants extracted from experimental data and ab initio calculations. In our approach, we did not assume any particular dominating magnetic model but we rather looked for all possible magnetic interactions in each compound. On the basis of a mixed B3LYP/broken symmetry (BS) approach (Section 2), a mapping of exchange constants between all pairs of adjacent vanadium sites has been considered. The influence of the coordination spheres of vanadium atoms on the calculated values was controlled by considering clusters of growing sizes (Section 3). It is well-known that the coupling constants are extremely sensitive to the local environment of magnetic centers. The comparison between values calculated on analogous cluster models is useful in determining magnetostructural trends in the five oxovanadium(IV) phosphate phases we considered. We also believed that our previous investigations of magnetostructural correlations in the three phases of $(VO)_2P_2O_7$ compound should be carried on the basis of recent experimental data on these five new oxovanadium(IV) phosphates.

2. Broken symmetry (BS) approach

A detailed description of the computational method used in this paper has been given elsewhere and is only briefly reviewed here [19,34–36].

The treatment of magnetic properties in polynuclear systems is generally achieved on the basis of a phenomenological Heisenberg–Dirac–Van Vleck spin hamiltonian (HDVV),

$$H = \sum_{\langle i,j \rangle} J_{ij} \mathbf{S_i} \cdot \mathbf{S_j}, \tag{1}$$

where $\langle i,j \rangle$ indicates summation over all i and j magnetic centers, $\mathbf{S_i}$ and $\mathbf{S_j}$ are the electronic spin operators at sites i and j and J_{ij} stands for the spin exchange constant. According to this equation, positive exchange constant means antiferromagnetic coupling between the two sites.

Let us consider a model system consisting of two magnetic centers with one unpaired electron each. In this case, Eq. (1) involves only one term and reads:

$$H = J_{12} \mathbf{S_1} \cdot \mathbf{S_2}. \tag{2}$$

It should be reminded that the phenomenological and quantum descriptions are related by $J_{12} = E_T - E_S$, where E_T and E_S are the energy of the triplet and singlet state, respectively. By use of the active electron approximation, it is usually admitted that such a description is valid for dimer systems containing more than two electrons. Thus, the study of magnetic properties usually requires the calculation of small energy differences in many electron systems. Considering the required degree of accuracy, several authors have put much efforts in multideterminantal methods [37–40]. However, this kind of calculations has a huge computation time cost and generally requires simplified geometrical structures.

An alternative approach based on the calculations of a broken symmetry (BS) state within the unrestricted DFT formalism has been proposed by Noodelman and Norman [41] and Noodelman [42]. In order to characterize the BS state, the equivalence between the two magnetic centers must be lifted. The spin symmetry is broken since the BS state is not a pure but a mixed spin state with $M_S = 0$. In fact, the electronic α- and β-densities are authorized to be different in space, and this difference is determined by the self-consistent field of the system in a density functional calculation. Therefore, both the geometrical and the spin symmetries are broken in this fictitious BS state. The resulting dimer exchange constant is linked to the energy of the triplet state (E_T) and the energy of the broken symmetry ($E_{\alpha\beta}$) state:

$$J_{12} = \frac{2(E_{\alpha\beta} - E_T)}{1 + S_{\alpha\beta}^2}, \tag{3}$$

where $S_{\alpha\beta}$ is the overlap integral between the magnetic α and β orbitals of the BS solution. As recently reported for model dimers of the vanadyl pyrophosphate structure, the overlap integrals between the magnetic orbitals are rather small and the localized limit of Eq. (3).

$$J_{12} = 2(E_{\alpha\beta} - E_T) \tag{4}$$

seems to be a satisfactory approximation. The BS state can then be reduced to a simple spin function $|\alpha\beta\rangle$.

Since we do not deal with molecular systems but with extended solids, a question arises about the validity of dimer models to describe the exchange interactions. In particular, it has been shown that three copper magnetic centers should be explicitly included when one aims to reproduce accurate exchange constants in the $CuGeO_3$ solid [43]. On the other hand, the analysis of clusters of higher nuclearity also allows to improve the description of the local environment. The methodology of BS states can be extended to polynuclear systems and be shortly detailed as follows. Not only one but several BS states can be constructed. Within the assumption of fully localized magnetic orbitals, the BS states are written as products of spin functions such as

$$|\alpha\alpha\beta\rangle = |\alpha\rangle|\alpha\rangle|\beta\rangle \tag{5}$$

for a three-interacting-site magnetic cluster. For such system, the HDVV hamiltonian reads

$$H = J_{12} \mathbf{S_1} \cdot \mathbf{S_2} + J_{23} \mathbf{S_2} \cdot \mathbf{S_3} + J_{31} \mathbf{S_3} \cdot \mathbf{S_1}. \tag{6}$$

On the basis of the spin functions, the diagonal elements of this Hamiltonian correspond to the BS states energies. The exchange parameters are linked to the

energies of the high-spin and the BS states:

$$2(E_{\mathrm{Smax}} - E_{\alpha\alpha\beta}) = J_{23} + J_{31},$$

$$2(E_{\mathrm{Smax}} - E_{\alpha\beta\alpha}) = J_{12} + J_{23},$$

$$2(E_{\mathrm{Smax}} - E_{\beta\alpha\alpha}) = J_{12} + J_{31}.$$

Similar expressions can be derived for four-nuclear clusters which were also considered in our study. However, for the sake of simplicity, we do not detail the corresponding relations.

All our calculations were performed using the Gaussian 98 package [44], with rather extended basis sets. Double-ζ GTO basis sets, namely 6-31G, were used for H, O, and P atoms, extended with one polarization function for P. As far as V atom is concerned, the effects of the core electrons up to $2p$ were accounted for with the Los Alamos pseudopotential. Double-ζ basis sets optimized for this particular effective core potential (ECP) were applied for the valence electrons. As in our earlier studies of the VPO phases, we used the standard generalized gradient-corrected hybrid functional B3LYP, consisting of the exchange Becke three-parameter functional and the Lee–Yang–Parr correlation one. As a starting point for the SCF procedure, the initial BS state was constructed by allowing the mixing of highest α and β spin-orbitals in the converged maximal spin state. The overlap integrals $S_{\alpha\beta}$ were computed by means of a local software that has been developed for specific Gaussian basis sets used in the Gaussian 98 package.

3. Description of molecular models

For the five oxovanadium phosphate phases, we did not assume a priori any dominating exchange pathway. Whatever the chemical nature of the bridge and the metal–metal distance, we explored all possible pairs of adjacent vanadium atoms. Four types of dimers can be identified in these phases depending on the connection between metallic sites. The notations suggested in the literature will be used in the following. D_O refers to the dimer in which two vanadium sites are connected by two μ-oxo bridges. The M and D_{OPO} dimers are characterized by one and two O–P–O connections, respectively. Finally, O label refers to μ-oxo-bridged dimers with one short and one long V–O bond. One should note that for the latter, the basal planes of the two VO_5 pyramids can be linked by additional oxygen–phosphorus bridges. Although the core part of each dimer type remains the same, two dimers can differ by the V–V distance, the geometries and the environments of the bridging ligands (valence and dihedral angles) and the relative orientation of the vanadyl groups. All studied dimers are listed in Table 2 and the corresponding molecular models are shown in Figs. 6–8.

Table 2
Model dimers considered for the different oxovanadium phosphates

Solid	Model dimer types
$VO(HPO_4)\cdot 0.5H_2O$	D_O^1, D_{OPO}^1, D_{OPO}^2, M^1
α-$VO(HPO_4)\cdot 2H_2O$	D_{OPO}^3, M^2, O^1
$VO(HPO_4)\cdot 4H_2O$	D_{OPO}^4, D_{OPO}^5, M^4
$VO(H_2PO_4)_2$	M^3, O^2
α-$VO(PO_3)_2$	D_{OPO}^6, O^3

One should stress that a single phase exhibits D_O dimer, namely the hemihydrate $VO(HPO_4)\cdot 0.5H_2O$ (Fig. 8a). Inspection of its structure in comparison to the vanadyl pyrophosphate $(VO)_2P_2O_7$ reflects the presence of one additional linkage between vanadium centers of D_O dimers through the oxygen atom of a water molecule. Two kinds of D_{OPO} dimers are present in this compound (Fig. 6). The first one (D_{OPO}^1) has a boat-like structure with the vanadyl bonds in syn-orthogonal configuration. The interchain coupling gives rise to a second kind of dimer(D_{OPO}^2) with anti-orthogonal configuration of the vanadyl bonds. The eight basal oxygen atoms of VO_5 pyramids lie approximately in the same plane. All other D_{OPO} dimers have a more or less pronounced chair-like structure and anti-orthogonal configuration of vanadyl bonds. The D_{OPO}^6 dimer is characterized not only by a more planar structure of the V$-(OPO)_2-$V fragment but also by the absence of water molecule in the basal planes of VO_5 pyramids. The M dimers strongly differ by the relative orientation of vanadyl bonds as well as by the presence of water molecules in the V coordination spheres (Fig. 7). Three kinds of O dimers are involved in quasi-linear chains of vanadyl bonds in α-$VO(HPO_4)\cdot 2H_2O$, $VO(H_2PO_4)_2$ and α-$VO(PO_3)_2$. Besides the bridging through μ-oxo bond, vanadium centers are also connected by one PO_4 bridge in the O^1 dimer (Fig. 8b), or hydrogen bonds in the O^2 dimer (Fig. 8c), or four P_3O_{10} fragments in the O^3 dimer (Fig. 8d).

The environments of magnetic vanadium atoms were explicitly included up to the third coordination spheres in each model dimer. The experimental structures were used without any optimization of the atomic positions. In order to ensure the electric neutrality of our model clusters, hydrogen atoms were attached to some oxygen atoms along the pre-existing bonds with a standard O–H distance 0.95 Å. As mentioned in the previous section, we also considered model clusters of higher nuclearities in order to assess the use of dimeric models in the calculation of exchange interactions in solids. These clusters are presented in the supplement. The estimations of exchange constants were performed on the basis of the theoretical framework detailed in Section 2. In the following section, we report the calculated values for all the different D_O, D_{OPO}, M and O dimer types.

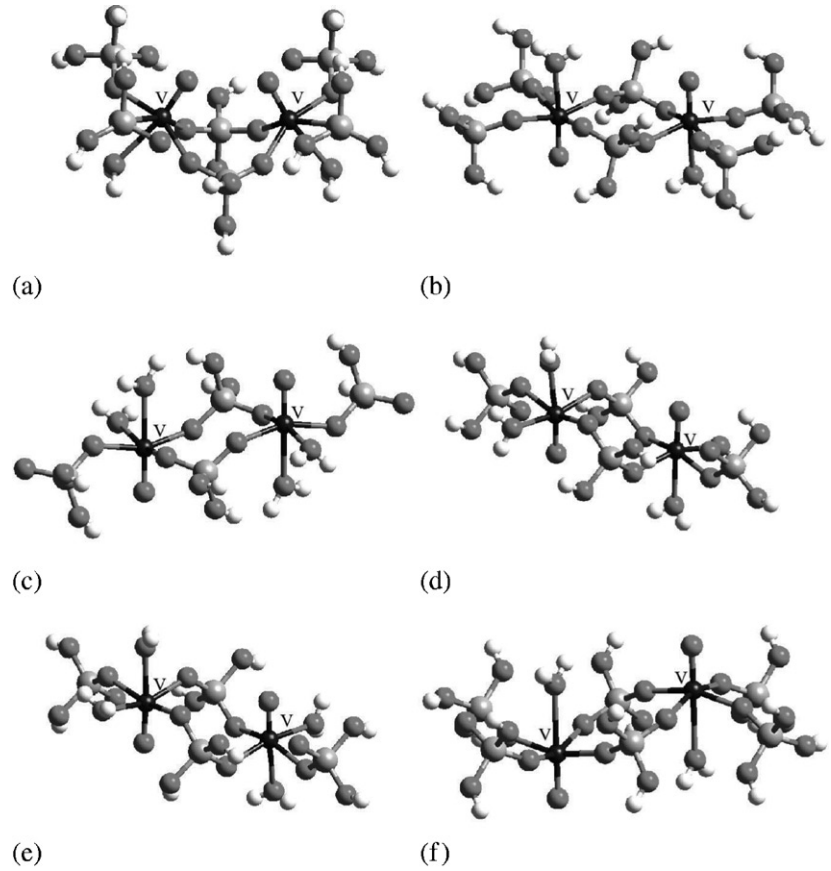

Fig. 6. D_{OPO}-type dimers: (a) D^1_{OPO}, (b) D^2_{OPO}, (c) D^3_{OPO}, (d) D^4_{OPO}, (e) D^5_{OPO} and (f) D^6_{OPO}.

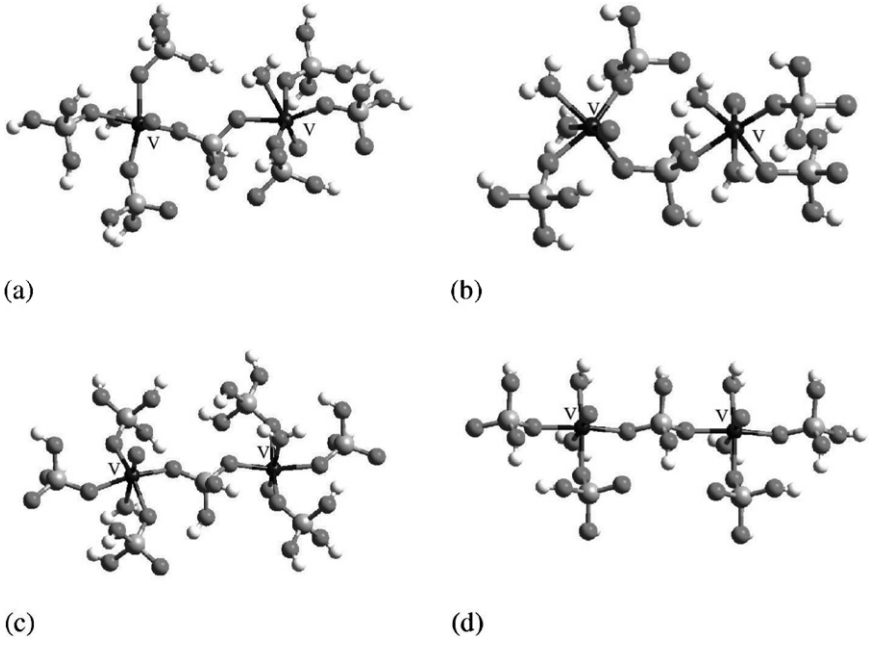

Fig. 7. M-type dimers: (a) M^1, (b) M^2, (c) M^3 and (d) M^4.

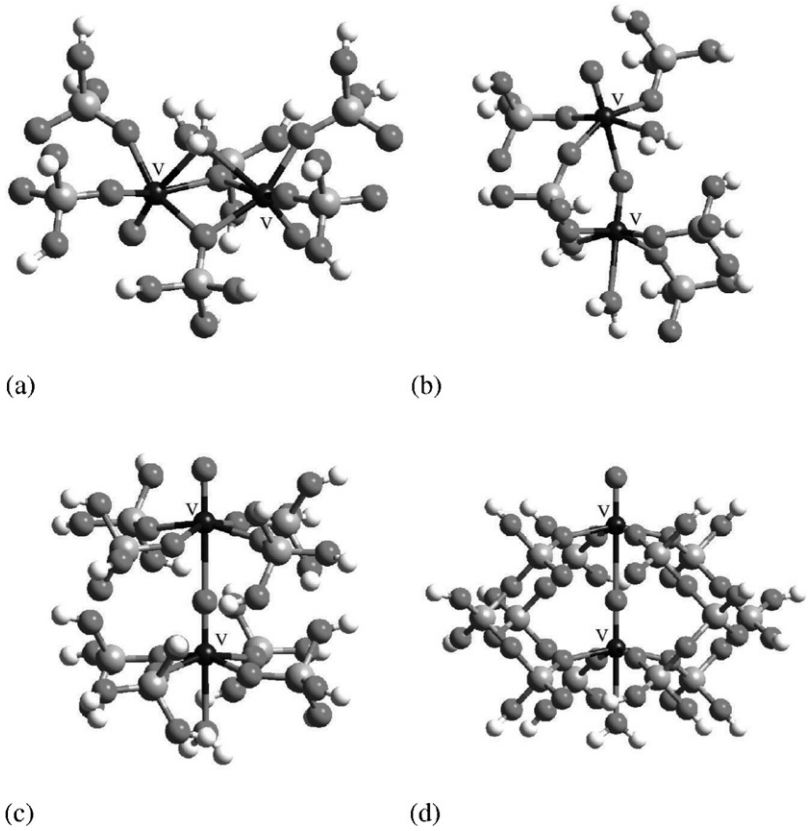

Fig. 8. D_O and O-type dimers: (a) D_O^1, (b) O^1, (c) O^2 and (d) O^3.

4. Results and discussion

4.1. Mapping of the exchange interactions

Exchange parameters values reported in the literature are mainly based on the analysis of the experimental magnetic susceptibility data [17]. It is clear that the choice of one particular model of magnetic interactions depicted by one Heisenberg hamiltonian directly controls the number and the values of the exchange parameters. Even if the spin model is reliable (for example, a dimer model), the attribution of the exchange constant to a particular pair of magnetic sites is not always obvious. Simple considerations based on the metal–metal distances are not always relevant. As observed in the vanadyl pyrophosphate phases, the dominant magnetic interaction occurs through the long O–P–O bridges, and not through the much shorter μ-oxo and vanadyl bond pathways. Therefore, theoretical approaches for the description of the exchange interactions in oxovanadium phosphates have become a powerful means of investigation. To our knowledge, a single theoretical study on the five oxovanadium phosphate compounds has been carried out on the basis of the EH method [12]. However, the main assumption in this approach states that only the antiferromagnetic contribution governs the total magnetic exchange variations. Even more, this antiferromagnetic part in different dimers is supposed to be completely defined by the HOMO–LUMO gap, a rather crude approximation [45]. In our study, we report original DFT calculations of exchange parameters for these compounds. The results for dimer molecular models are summarized in Table 3 whereas the ones for the extended models are given in the supplement.

As we see for the hemihydrate phase, the most important antiferromagnetic exchange interaction is provided by D_{OPO}^1 dimer (122 K). However, the interaction through μ-oxo bridge has a comparable value (77 K) and is also of antiferromagnetic nature. Keeping in mind the position of these two types of dimers in the crystal lattice, we see that these results are consistent with an alternating antiferromagnetic spin chain model. Conversely, the inter-chain interactions described by D_{OPO}^2 and M^1 dimers are weaker in amplitude and of ferromagnetic nature. As mentioned in the Introduction, the susceptibility and INS data were described on the basis of an isolated dimer model. However, agreement between these sets of experimental data was not reached since the dominating exchange pathway was attributed to D_O and D_{OPO} for the susceptibility and the INS data, respectively.

Table 3
Calculated exchange parameters

Solid	J(K)			
	D_O	D_{OPO}	M	O
$VO(HPO_4)\cdot 0.5H_2O$	77	122 (D^1_{OPO}) −8 (D^2_{OPO})	−3	
α-$VO(HPO_4)\cdot 2H_2O$		67	2	−11
$VO(HPO_4)\cdot 4H_2O$		−11 (D^4_{OPO}) −12 (D^5_{OPO})	19	
$VO(H_2PO_4)_2$			2	−18
α-$VO(PO_3)_2$		12		−13

Nevertheless, the latest NMR measurements evidenced one-dimensional coupling between these different dimers D_O and D_{OPO}, suggestive of an alternating dimer chain model [7]. From our results, the coexistence of two main exchange parameters agrees with this recent observation on the $VO(HPO_4)\cdot 0.5H_2O$ compound.

Calculations on the dihydrate oxovanadium phosphate α-$VO(HPO_4)\cdot 2H_2O$ justify the use of an isolated dimer model for the description of magnetic properties. In agreement with previous studies, we conclude that the dominant exchange pathway should be attributed to the D_{OPO} dimer found in this compound (D^3_{OPO}). The calculated exchange parameter value 67 K is in relatively good agreement with the experimental value 46 K based on the isolated dimer model. In the light of our theoretical estimations, a better description of the magnetic interactions would be achieved if one includes the weak ferromagnetic interaction (−11 K) described by the O^1 dimer.

In $VO(HPO_4)\cdot 4H_2O$ compound, one cannot identify any dominating exchange constant. The exchange pathway in the M dimer leads to an antiferromagnetic interaction (19 K) of the same order in absolute value as the ferromagnetic interactions (−11 and −12 K) in both D_{OPO} dimers. We believe that the zigzag chain model which has been used previously to analyze the magnetic susceptibility data is not suitable. The simplest approach should include three different paths of magnetic interactions by means of one M (M^4) and two D_{OPO} dimers (D^4_{OPO} and D^5_{OPO}).

Finally, $VO(H_2PO_4)_2$ and α-$VO(PO_3)_2$ phases exhibit very similar magnetic behavior. Ferromagnetic O-type dimer chains (O^2, −13 K and O^3, −18 K) are organized along the **c**- and **b**-axis, respectively. Each chain is antiferromagnetically coupled (M^3, 2 K and D^6_{OPO}, 12 K) to the nearest neighbor chains by either a single O–P–O or two O–P–O bridges in $VO(H_2PO_4)_2$ and α-$VO(PO_3)_2$ phases, respectively. Even though the values (ferromagnetic) we found in O dimers are small and of opposite sign from what has been suggested in the literature, they agree with our previous calculations for the similar dimers in $(VO)_2P_2O_7$. The apparent disagreement between calculated and experimental exchange parameters in Refs. [3,31] needs further investigations for the $VO(H_2PO_4)_2$ (O^2) phase. In particular, we should note that the chemical shift value 5 ppm [3] also strongly differs from the value found in a more recent study, 2245 ppm [46].

Since we were also interested in considering the influence of the local environments of magnetic centers, cluster models of larger sizes were investigated (Supplement). The HPO phase of $(VO)_2P_2O_7$ was used to tackle this important issue. In our previous study, we reported calculations on this particular compound based on a dimer approach [19]. The four types of dimer D_O, D_{OPO}, M and O are met simultaneously and rather large values of exchange constants have been estimated. Thus, we believe that the interdimer interactions might not be negligible and the coordination spheres should be extended. A trimeric approach involving two types of dimer was not found to be a satisfactory since asymmetry between the magnetic sites is then introduced. If one considers a tetramer, the symmetry between the two magnetic centers of the central dimeric unit is retained as it exists in the solid. Again, it should be recalled that exchange values are very sensitive to the modeling of the environment. Since variations of less than 10% relative to the dimer values are observed in our calculations of exchange parameters in tetrameric clusters, we may conclude that the dimer model approach is reliable enough for this particular class of compounds.

4.2. Magnetostructural correlations

In the previous section, we detailed the different possible exchange pathways and the corresponding exchange constants values within each phase. Originally, our purpose was also to look into a variety of similar compounds in order to identify the structural parameters that may account for the exchange constants variations. In agreement with our previous study [19] of the three $(VO)_2P_2O_7$ phases, the most efficient exchange path is observed when two O–P–O units bridge the magnetic centers (D_{OPO} dimers). However, as a result of structural changes, the exchange constant in D_{OPO} dimers may be comparable or even less than the ones we calculated in other types of dimer. Following the analysis suggested by Roca et al. [12], one can identify two geometrical parameters that strongly correlate to the exchange values. The in-plane shearing of the basal parts of the two VO_5 pyramids (Fig. 9a) reduces the antiferromagnetic interactions, leading for strong enough distortions to a ferromagnetic coupling. We believe that the ferromagnetic nature of this interchain interaction may result from the break of the two O–P–O connections. The intercenter interaction is then mainly provided by the $O_1\cdots O_2$ contact. The magnetic pathway in this class of compounds is also very sensitive to

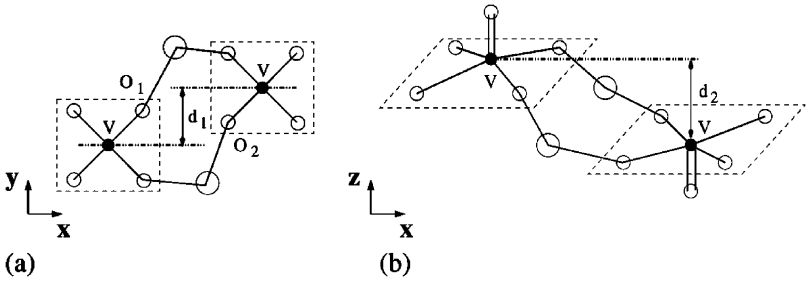

Fig. 9. Two structural characteristic: (a) the d_1 parameter and (b) the d_2 distance. Each square shows the basal plane of each VO_5 pyramid.

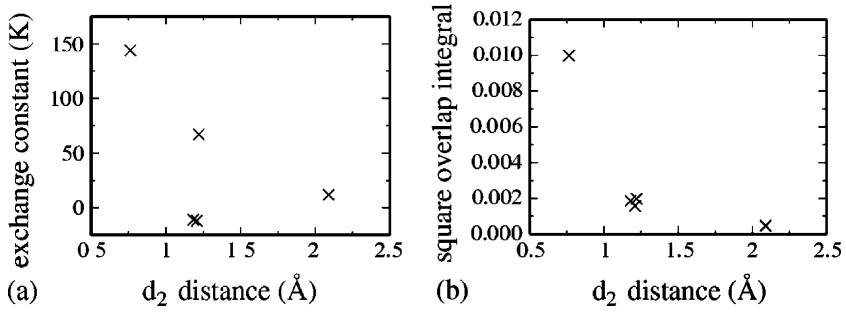

Fig. 10. (a) Exchange constant variations as a function of d_2 distance; (b) Square of overlap of the magnetic orbitals as a function of d_2 distance.

another structural characteristic (Fig. 9b). The relative displacements of the two VO_5 pyramids along the vanadyl bond direction in D_{OPO} dimers lead to chair-like structures mentioned before. As main trend, the exchange constant decreases with the distance d_2 (Fig. 10a). The physical origin of such influence lies in the fact that as the two moieties are moved apart, the overlap between the magnetic orbitals is reduced by a factor of almost 20 (Fig. 10b). Thus, the antiferromagnetic contribution decreases and so does the overall magnetic coupling. The apparent singularity observed in the D_{OPO} dimers of $VO(HPO_4)\cdot 4H_2O$ phase (-11 K for D^4_{OPO} and -12 K for D^5_{OPO}) is explained by a shorter V–V distance, resulting in a larger direct exchange interaction of ferromagnetic type.

From our calculations, changes in the exchange coupling in M dimers, M^3 and M^4, can be understood from the variations of the dihedral angles θ, characterizing the position of the bridging phosphorus atom with respect to the vanadyl oxygen atom. In M^4 dimer, θ is almost zero and gives rise to a local symmetry plane. The pi-overlap between the two oxygen atoms $2p$ orbitals of the O–P–O bridges is mainly responsible for the magnetic transfer. Conversely, in M^3 the phosphorus atom does not lie in the plane of vanadyl groups ($\theta = 82°$), introducing a mixing between the oxygen contracted $2s$ and diffuse $2p$ orbitals. The net effect is a reduction of the overlap between the magnetic orbitals and of the antiferromagnetic contribution. Thus, the exchange value is smaller in M^3 (2 K) than in M^4 (19 K). In M^1 and M^2 the two vanadyl bonds are neither parallel nor orthogonal. The resulting weak overlap is reflected by small (about 0 K) exchange constants.

5. Conclusion

In this study, we showed that the molecular dimer model approach was suitable for the analysis of exchange interactions in a variety of oxovanadium phosphate solids. Special attention was paid to the local environments of magnetic centers. However, we observed that increasing the metallic nuclearity of the model clusters does not lead to any significant changes in the exchange constant estimation.

Even though the connections between magnetic sites are chemically quite similar, a wide range of exchange parameters was determined. As in our previous study of the oxovanadium phosphate compounds, our calculations revealed that small modifications of the local structure modulate the magnetic interactions.

In the light of these calculations, different spin models were proposed for the analysis of magnetic properties. For $VO(HPO_4)\cdot 0.5H_2O$, $VO(HPO_4)\cdot 4H_2O$, $VO(H_2PO_4)_2$ and α-$VO(PO_3)_2$ solids, our models differ from the ones which had been suggested in the literature. In α-$VO(HPO_4)\cdot 2H_2O$, the isolated dimer model might be considered as a good starting point, even though one additional ferromagnetic interaction should improve the description.

In a future paper, we intend to use these theoretically defined constants to analyze the temperature-dependent paramagnetic shifts in ^{31}P NMR spectra.

References

[1] J.W. Johnson, D.C. Johnston, A.J. Jacobson, J.F. Brody, J. Am. Chem. Soc. 106 (1984) 8123.
[2] J.T. Wrobleski, Inorg. Chem. 27 (1988) 946.
[3] D. Beltrán-Porter, A. Beltrán-Porter, P. Amorós, R. Ibañez, E. Martinez, A. Le Bail, G. Ferrey, G. Villeuneuve, Eur. J. Solid State Inorg. Chem. 28 (1991) 131.
[4] M.T. Sananes, A. Tuel, J. Chem. Soc. Chem. Commun. 13 (1995) 1323.
[5] M.T. Sananes, A. Tuel, Solid State Nucl. Magn. Reson. 6 (1996) 157.
[6] D.A. Tennant, S.E. Nagler, A.W. Garrett, T. Barnes, C.C. Torardi, Phys. Rev. Lett. 78 (1997) 4998.
[7] J. Kikuchi, T. Aoki, K. Motoya, T. Yamauchi, Y. Ueda, Physica B 284 (2000) 1481.
[8] D.C. Johnston, J.W. Johnson, D.P. Goshorn, A.J. Jacobson, Phys. Rev. B 35 (1987) 219.
[9] P. Amorós, A. Beltrán, D. Beltrán, J. Alloys Compd. 188 (1992) 123.
[10] T. Barnes, J. Riera, Phys. Rev. B 50 (1994) 6817.
[11] A.W. Garrett, S.E. Nagler, D.A. Tennant, B.C. Sales, T. Barnes, Phys. Rev. Lett. 79 (1997) 745.
[12] M. Roca, P. Amorós, J. Cano, M.D. Marcos, J. Alamo, A. Beltrán-Porter, D. Beltrán-Porter, Inorg. Chem. 37 (1998) 3167.
[13] J. Kikuchi, K. Motoya, T. Yamauchi, Y. Ueda, Phys. Rev. B 60 (1999) 6731.
[14] H.J. Koo, M.H. Whangbo, Inorg. Chem. 39 (2000) 3599.
[15] L.M. Lawson Daku, S.A. Borshch, V. Robert, B. Bigot, Chem. Phys. Lett. 330 (2000) 423.
[16] L.M. Lawson Daku, S.A. Borshch, V. Robert, B. Bigot, Phys. Rev. B 63 (2001) 174439.
[17] D.C. Johnston, T. Saito, M. Azuma, M. Takano, T. Yamauchi, Y. Ueda, Phys. Rev. B 64 (2001) 134403.
[18] G.S. Uhrig, B. Normand, Phys. Rev. B 63 (2001) 134418.
[19] S. Petit, S.A. Borshch, V. Robert, J. Am. Chem. Soc. 124 (2002) 1744.
[20] G. Centi, Catal. Today (Special Issue) 16 (1993) 1.
[21] F. Trifiro, G. Centi, J.R. Ebner, V.M. Franchetti, Chem. Rev. 88 (1988) 55.
[22] E. Bordes, Catal. Today 1 (1987) 499.
[23] J.M. Mouesca, L. Noodleman, D.A. Case, B. Lamotte, Inorg. Chem. 34 (1995) 4347.
[24] Y.E. Gorbunova, S.A. Linde, Sov. Phys. Dokl. 24 (1979) 138.
[25] V.V. Guliants, S.A. Holmes, J.B. Benziger, P. Heaney, D. Yates, I.E. Wachs, J. Mol. Catal. A 172 (2001) 265.
[26] H. Worzala, T. Goetze, D. Fratzky, M. Meisel, Acta Crystallogr. Sect. C 54 (1998) 283.
[27] S.A. Linde, Y.E. Gorbunova, A.V. Lavrov, Y.G. Kustnetsov, Dokl. Akad. Nauk SSSR 244 (1979) 1411.
[28] E.V. Murashova, N.N. Chudinova, Kristallografiya 39 (1994) 145.
[29] D. Fratzky, H. Worzala, T. Goetze, M. Meisel, Z. Kristallogr.—New Cryst. Struct. 214 (1999) 9.
[30] G. Villeneuve, K.S. Suh, P. Amorós, N. Casañ-Pastor, D. Beltrán-Porter, Chem. Mater. 4 (1992) 108.
[31] J. Kikuchi, N. Kurata, K. Motoya, T. Yamauchi, Y. Ueda, J. Phys. Soc. Jpn 70 (2001) 2765.
[32] S. Geupel, K. Pilz, S. Van Smaalen, F. Büllesfeld, A. Prokofiev, W. Assmus, Acta Crystallogr. Sect. C 58 (2002) i9.
[33] H.J. Koo, M.H. Whangbo, P.D. VerNooy, C.C. Torardi, W.J. Marshall, Inorg. Chem., in press.
[34] L. Noodleman, D.A. Case, Adv. Inorg. Chem. 38 (1992) 423.
[35] R. Caballol, O. Castell, F. Illas, I. de P.R. Moreira, J.P. Malrieu, J. Phys. Chem. A 101 (1997) 7860.
[36] E. Ruiz, J. Cano, S. Alvarez, P. Alemany, J. Comput. Chem. 20 (1999) 1391.
[37] P. de Loth, P. Cassoux, J.P. Daudey, J.P. Malrieu, J. Am. Chem. Soc. 103 (1981) 4007.
[38] C. de Graaf, C. Sousa, I. de P.R. Moreira, F. Illas, J. Phys. Chem. A 105 (2001) 11371.
[39] C.J. Calzado, J. Cabrero, J.P. Malrieu, R. Caballol, J. Chem. Phys. 116 (2002) 2728.
[40] C.J. Calzado, J. Cabrero, J.P. Malrieu, R. Caballol, J. Chem. Phys. 116 (2002) 3985.
[41] L. Noodleman, J.G. Norman, J. Chem. Phys. 70 (1979) 4903.
[42] L. Noodleman, J. Chem. Phys. 74 (1981) 5737.
[43] E. Ruiz, J. Cano, S. Alvarez, P. Alemany, M. Vergaguer, Phys. Rev. B 61 (2000) 54.
[44] M.J. Frisch, G.W. Trucks, H.B. Schlegel, G.E. Scuseria, M.A. Robb, J.R. Cheeseman, V.G. Zakrzewski, R.E. Montgomery, J.A. Stratmann, J.C. Buran, S. Dapprich, J.M. Millam, A.D. Daniels, K.N. Kudin, M.C. Strain, O. Farkas, J. Tomasi, V. Barone, M. Cossi, R. Cammi, C. Mennuci, B. Pomelli, C. Adamo, S. Clifford, J. Ochterski, G.A. Peterson, P.Y. Ayala, Q. Cui, K. Mokuma, D.K. Malick, A.D. Rabuk, K. Raghavachari, J.B. Foresman, J. Cioslowski, J.V. Ortiz, B.B. Stefanov, G. Liu, A. Liashenko, P. Piskorz, I. Komaromi, R. Gomperts, R.L. Martin, D.J. Fox, T. Keith, M.A. Al-Laham, C.Y. Peng, A. Nanayakkara, C. Gonzalez, M. Challacombe, P.M.W. Gill, B.G. Johnson, W. Chen, M.W. Wong, J.L. Andres, M. Head-Gordon, E.S. Replogle, J.A. Pople, Gaussian 98 Revision A. 7: Gaussian, Inc., Pittsburgh, PA.
[45] P.J. Hay, J.C. Thibeault, R.J. Hoffmann, J. Am. Chem. Soc. 97 (1975) 4884.
[46] A. Tuel, M.T. Sananes-Schulz, J.C. Volta, Catal. Today 37 (1997) 59.